Electronic Supplementary Material (ESI) for Organic & Biomolecular Chemistry.

Tetrathiafulvalene mono- and bis-1,2,3-triazole precursors by click chemistry: structural diversity and reactivity

Thomas Biet and Narcis Avarvari*

SUPPORTING INFORMATION

X-Ray structures

Compound **2**

Table S1. Selected lengths (Å) and angles (º) for **2**

Distances (Å)		Torsion Angle (º) (calc)		Dihedral Angle between two planes(º) (calc)
C(3)-C(4)	1.260(4)	C(6)-C(5)-C(7)-C(8)	6.32	S(3)-C(4)-S(4)-C(5)-C(6) & C(7)-N(3)-N(1)-N(2)-C(8) 6.00
S-C int.	1.702(4)	C(6)-C(5)-C(7)-N(1)	5.93	
C(1)-C(2)	1.304(5)			
C(5)-C(6)	1.319(5)			
C(7)-C(8)	1.348(5)			
C(.)-N(.)	1.274(5)			
N(1)-N(2)	1.347(4)			
N(2)-N(3)	1.204(4)			

Intermolecular contacts: S1-S1: 3.51 Å; N2-H6 : 2.83 Å; N3-H6 : 2.84 Å; N3-H13A: 2.89 Å.

Compound **5**

Table S2. Crystal Data and Structure Refinement for **5.**

empirical formula	$C_{18}H_{24}S_4Si_2$
fw	424.79
T (K)	293(2)
wavelength (Å)	0.71073
cryst syst	triclinic
space group	*P-1*
unit cell dimens	
a (Å)	6.3081 (14)
b (Å)	8.1474 (16)
c (Å)	22.670 (5)
α(deg)	94.79 (3)
β(deg)	96.73 (2)
γ(deg)	92.57 (2)
V (Å^3)	1151.3 (4)
Z	2
D_c (g cm^{-3})	1.225
abs coeff (mm^{-1})	0.516
F(000)	448
cryst size (mm^3)	0.5 × 0.1 × 0.02
θ range for data collection (deg)	3.87–22.99
limiting indices	$-6 \le h \le 6$,
	$-8 \le k \le 8$,
	$-23 \le l \le 24$
reflns collected	12528
indep reflns	3148
completeness (%) to θ = 25.59°	98.9
abs correction	
refinement method	full-matrix least squares on F^2
data/restraints/param	3148/0/217
GOF on F^2	1.072
final R indices [$I > 2\sigma(I)$]	R1 = 0.0555, wR2 = 0.0943
R indices (all data)	R1 = 0.1165, wR2 = 0.1139
largest diff. peak and hole (e Å^{-3})	0.305 and –0.256

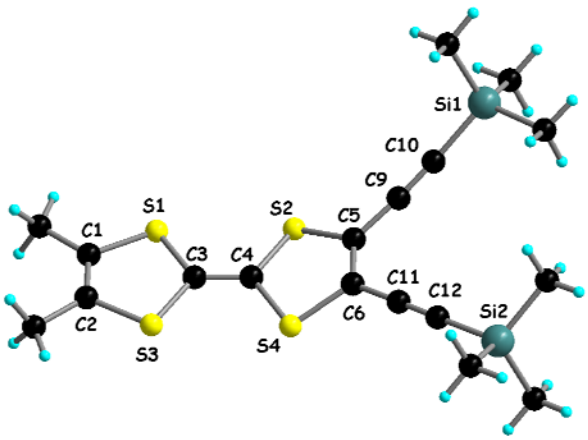

Fig. S1 Molecular structure of **5**.

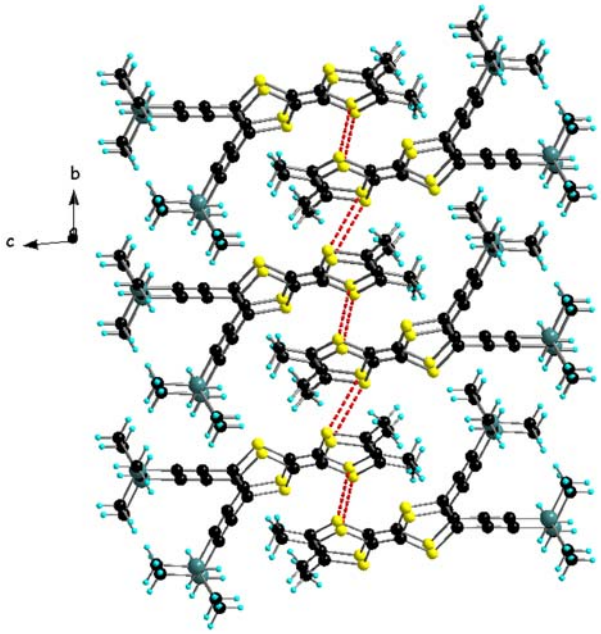

Fig. S2 Packing of molecules in the structure of **5** with an emphasis on the S···S contacts.

Table S3. Selected lengths (Å) and angles (º) for **5**

Distances (Å)		Torsion Angle (º) (calc)	Dihedral Angle between two planes(º) (calc)
C(3)-C(4)	1.344(7)		S(3)-C(4)-S(4) & S(3)-S(4)-C(5)-C(6) 22.62
S-C int.	1.756(5)		
C(1)-C(2)	1.346(8)		
C(5)-C(6)	1.340(7)		
C(7)-C(9)	1.205(7)		
C(8)-C(10)	1.189(7)		
C(9)-Si(2)	1.828(6)		
C(10)-Si(1)	1.848(7)		

Intermolecular contacts: S1-S1: 3.89 Å; S3-S3: 3.90 Å.

Compound **8**

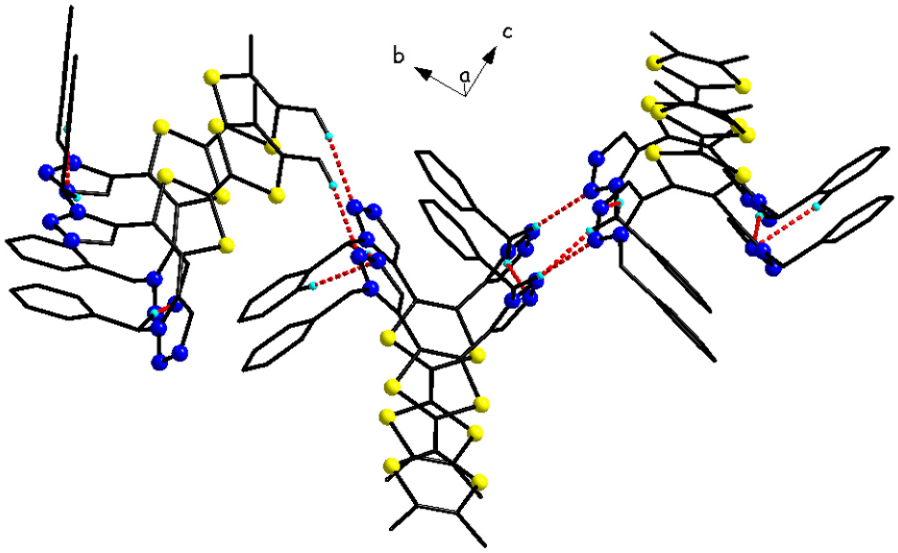

Fig. S3 Packing of molecules in the structure of **8** with an emphasis on the N···H contacts.

Table S4. Selected lengths (Å) and angles (º) for **8**

Distances (Å)		Torsion Angle (º) (calc)		Dihedral Angle between two planes(º) (calc)
C(3)-C(4)	1.334(5)	C(6)-C(5)-C(7)-C(8)	87.13	S(3)-C(4)-S(4)-C(5)-C(6) & C(7)-N(3)-N(1)-N(2)-C(8) 88.75
S-C int.	1.757(4)	C(6)-C(5)-C(7)-N(1)	87.66	
C(1)-C(2)	1.322(6)			
C(5)-C(6)	1.347(5)	C(5)-C(6)-C(9)-C(10)	37.66	S(3)-C(4)-S(4)-C(5)-C(6) & C(9)-N(4)-N(5)-N(6)-C(10) 41.34
C(7)-C(8)	1.367(6)	C(5)-C(6)-C(9)-N(4)	41.45	
C(.)-N(.)	1.346(6)			
N(1)-N(2)	1.339(5)			
N(2)-N(3)	1.301(5)			
C(9)-C(10)	1.372(6)			
C(.)-N(.)	1.350(5)			
N(4)-N(5)	1.346(5)			
N(5)-N(6)	1.307(5)			

Intermolecular contacts: N2-H13A : 2.43 Å; N6-H20B : 2.68 Å; N6-H26 : 2.59 Å; N5-H11A: 2.69 Å, N3-H13B: 2.82 Å.

Compound **9**

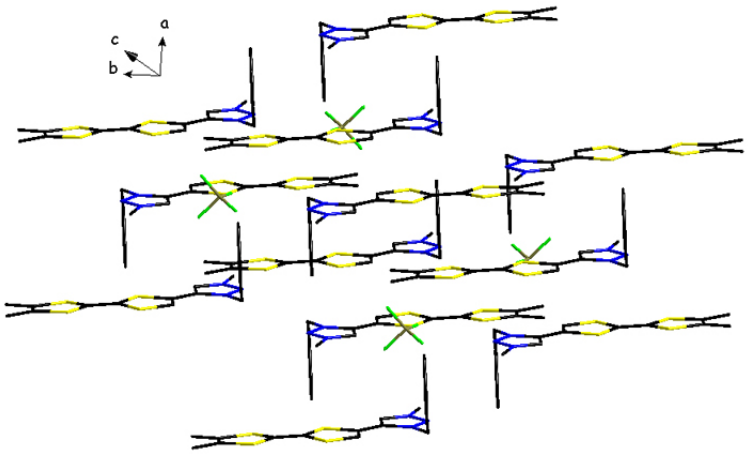

Fig. S4 Packing of molecules in the structure of **9**.

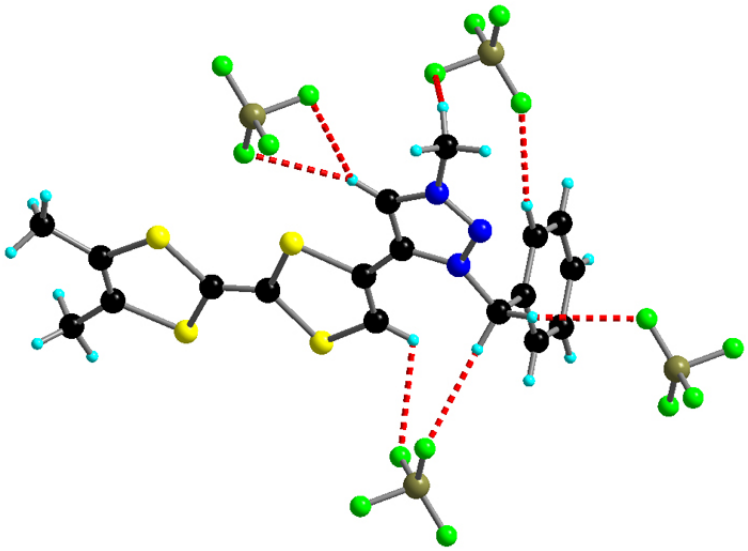

Fig. S5 F···H hydrogen bonding in the structure of **9**.

Table S5. Selected lengths (Å) and angles (º) for **9**

Distances (Å)		Torsion Angle (º) (calc)		Dihedral Angle between two planes(º) (calc)
C(3)-C(4)	1.351(4)	C(6)-C(5)-C(7)-C(8)	1.62	S(3)-C(4)-S(4)-C(5)-C(6) & C(7)-N(3)-N(1)-N(2)-C(8) 2.29
S-C int.	1.754(3)	C(6)-C(5)-C(7)-N(1)	3.25	
C(1)-C(2)	1.332(5)			
C(5)-C(6)	1.339(5)			
C(7)-C(8)	1.375(5)			
C(.)-N(.)	1.356(4)			
N(1)-N(2)	1.326(4)			
N(2)-N(3)	1.306(4)			
C(18)-N(3)	1.468(5)			

Intermolecular contacts: F2-H6 : 2.63 Å; F4-H11A : 2.51 Å; H8-F1 : 2.49 Å; H8-F4 : 2.53Å; H11B-F3 : 2.55 Å; H13-F3 : 2.39 Å; H18C-F1 : 2.62 Å.

Electrochemical studies. Cyclic voltammetry measurements were performed using a three-electrode cell equipped with a platinum millielectrode of 0.126 cm^2 area, an Ag/Ag^+ pseudo-reference and a platinum wire counter-electrode. The potential values were then re-adjusted with respect to the saturated calomel electrode (SCE). The electrolytic media involved a 0.1 $mol.L^{-1}$ solution of $(n\text{-}Bu)_4NPF_6$ in CH_2Cl_2. All experiments have been performed at room temperature at 0.1 $V{\cdot}s^{-1}$. Experiments have been carried out with an EGG PAR 273A potentiostat with positive feedback compensation.

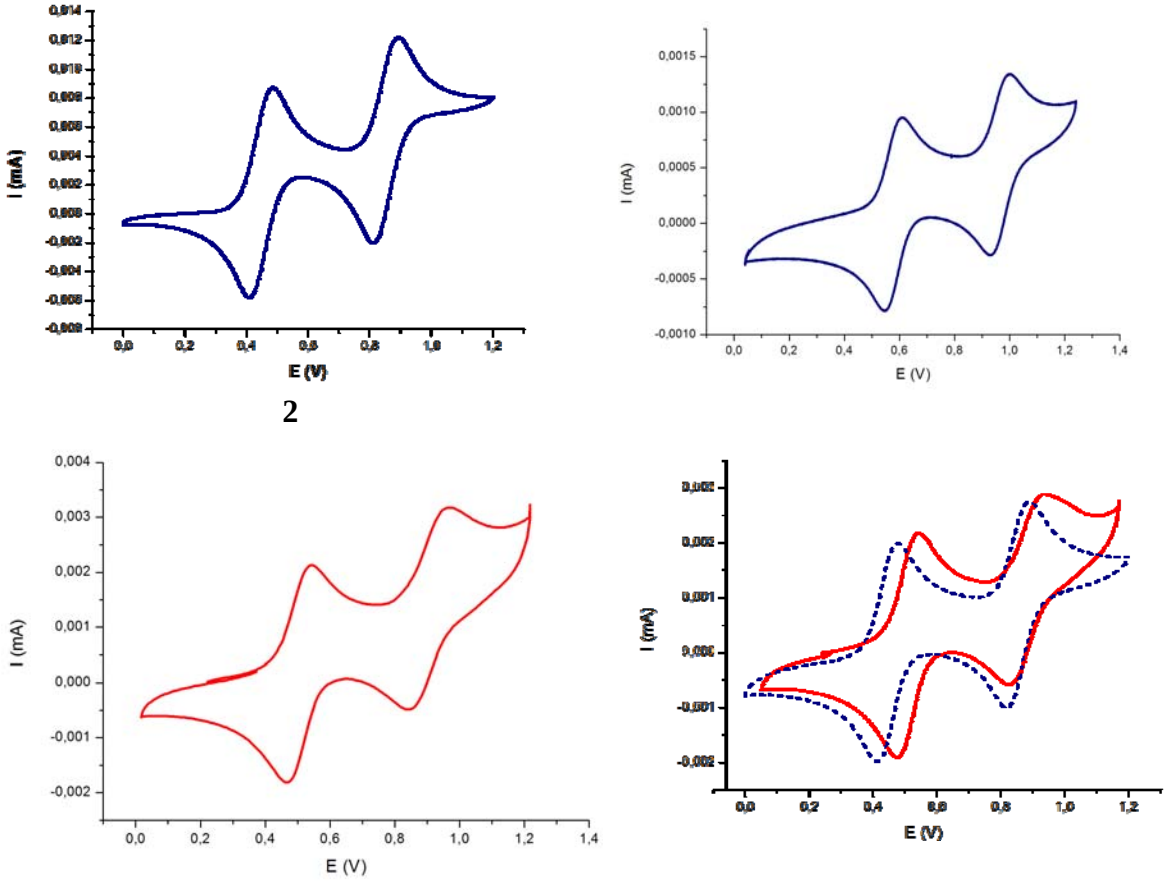

Fig. S6 Cyclic voltammograms.

Table S6. Oxidation potentials from cyclic voltammetry data. Measurements have been performed in CH_2Cl_2 in the presence of $(n\text{-}Bu_4N)PF_6$ (0.1 M) at a scan rate of 0.1 $V{\cdot}s^{-1}$.

compound	$E^1_{1/2}$ (V)	$E^2_{1/2}$ (V)
2	0.45	0.85
1	0.44	0.85
9	0.51	0.91
8	0.57	0.96

UV-Vis spectra of CH_2Cl_2 solutions

2 (10^{-4} M)

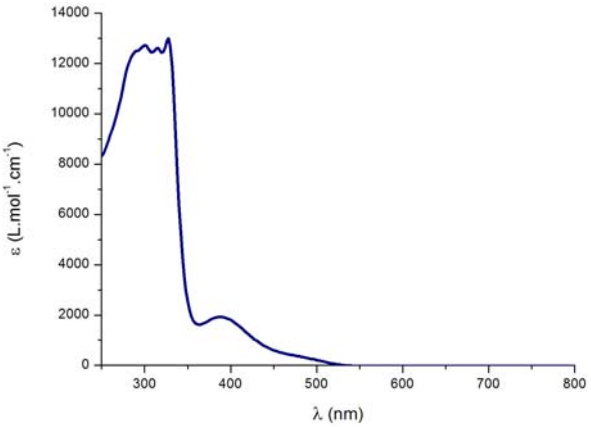

1 (10^{-5} M)

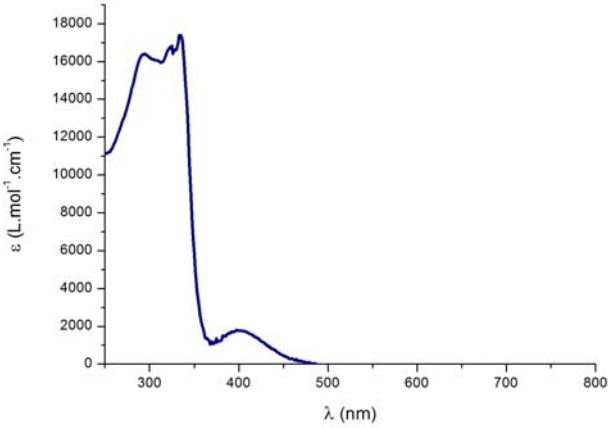

9 (10^{-4} M)

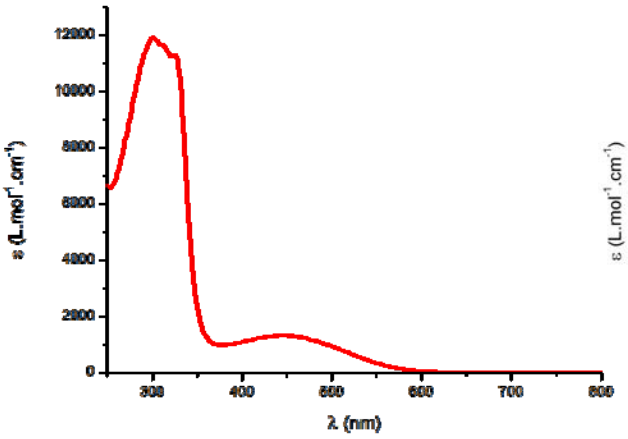

1 + 9 (10^{-4} M)

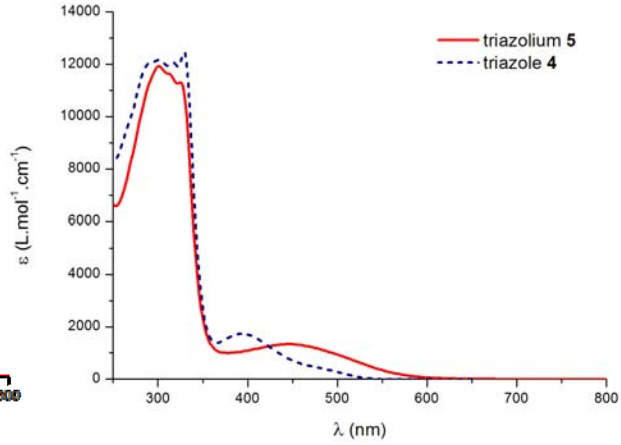

Fig. S7 UV-Vis spectra.

Table S7. UV-Vis data.

compound	λ_{max} (nm)	ε (L.mol^{-1}.cm^{-1})
2	388	1967
1	394	1758
9	451	1343

UV-Vis of 1 with HBF_4 in CH_2Cl_2 (10^{-4} M)

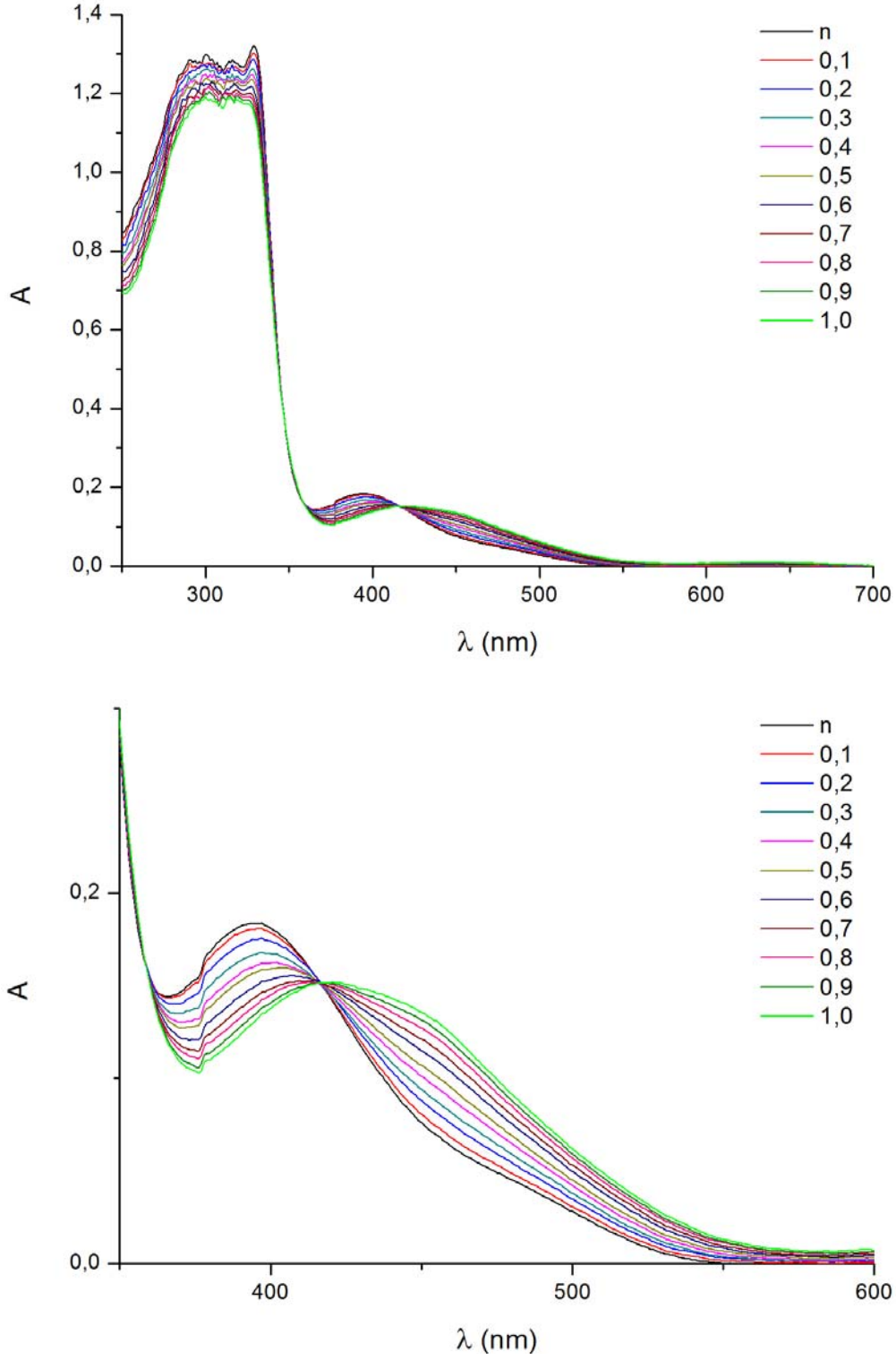

Fig. S8 Acidic titration of **1**. Isosbestic points : λ = 358 nm, A = 0.163; λ = 416 nm, A = 0.151

UV-Vis of 8 with HBF_4 in CH_2Cl_2 (10^{-4} M)

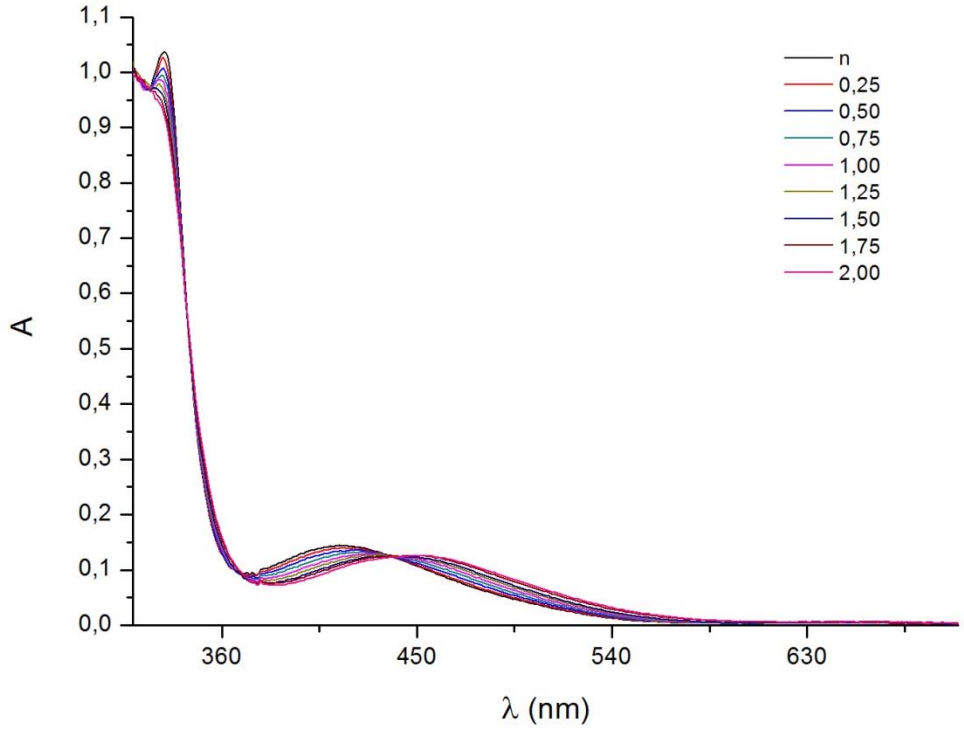

Zoom

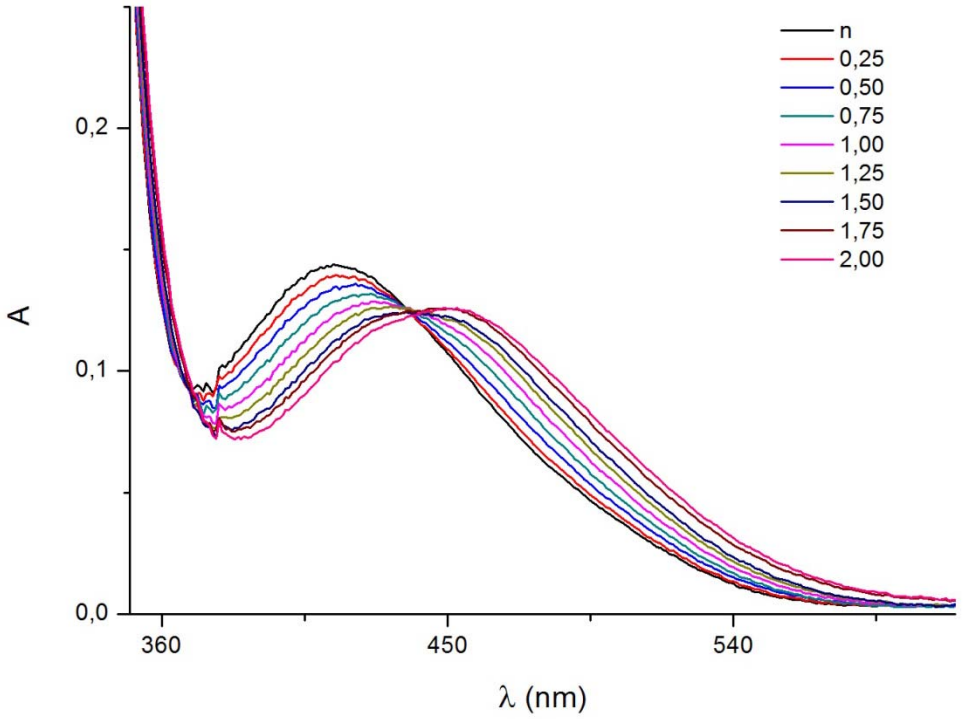

Zoom 0→1eq.

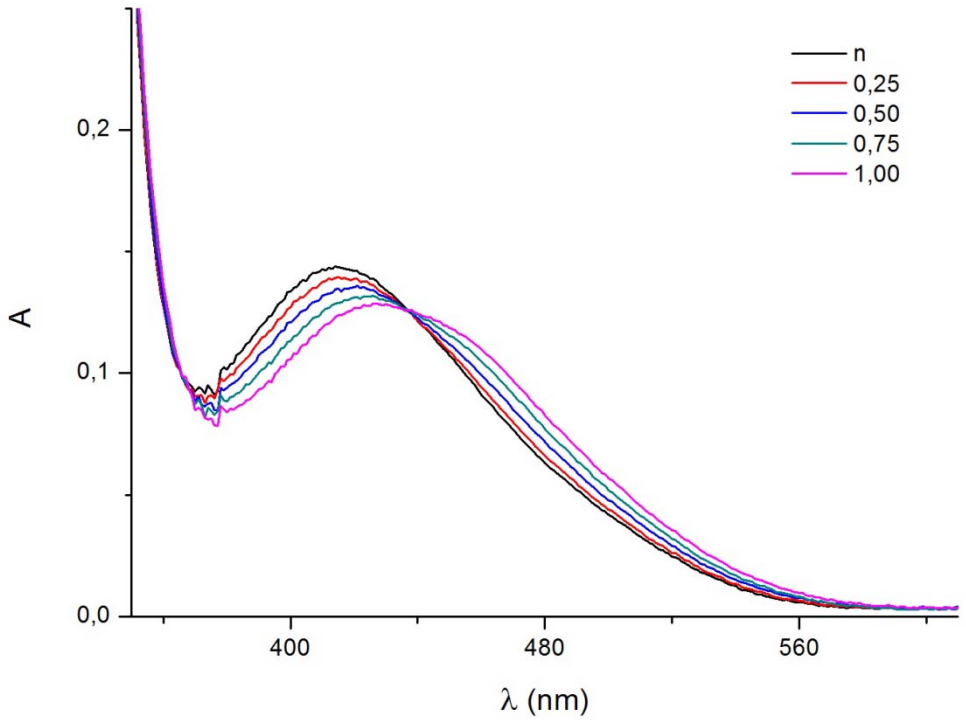

Zoom 1→2eq.

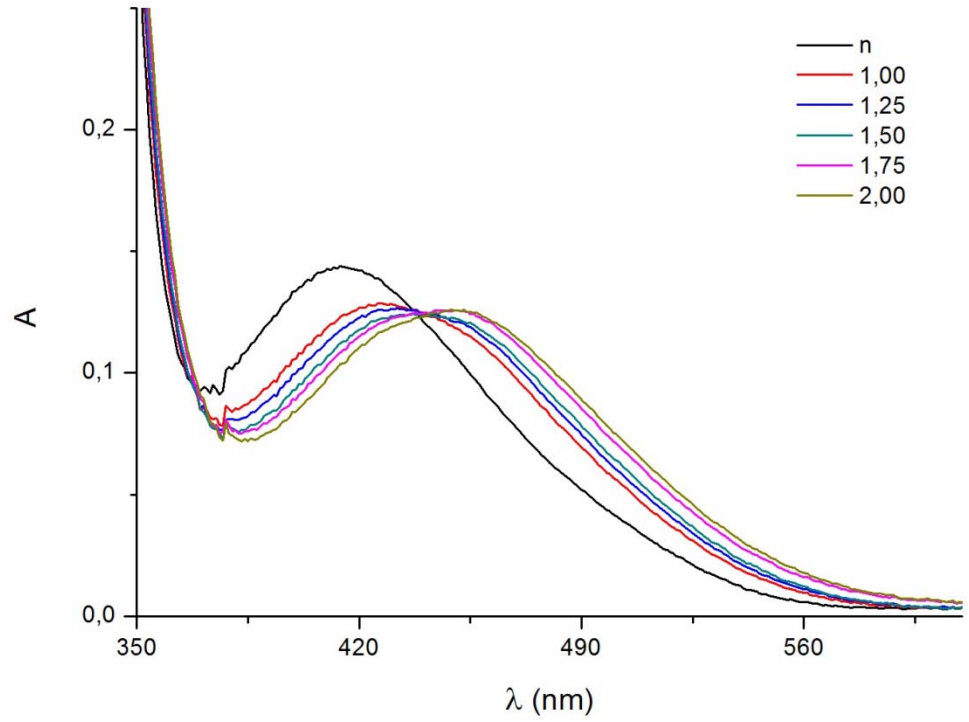

Fig. S9 Acidic titration of **8**. Neutral : λ = 415 nm, A = 0.143, ε = 1430 $L.mol^{-1}.cm^{-1}$. Isosbestic points : λ = 437 nm, A = 0.126; λ = 442 nm, A = 0.124.